Preprints, 10th IFAC International Symposium on
Advances in Automotive Control
Columbus, Ohio, USA, August 28-30, 2022

Challenges of a Fast Diagnostic to Inform Screening of Retired Batteries

Joseph A. Drallmeier * **Clement Wong** * **Charles E. Solbrig** *
Jason B. Siegel * **Anna G. Stefanopoulou** *

* *Battery Controls Group, University of Michigan, Ann Arbor, MI, 48109 USA. (e-mail: drallmei, clemwong, csolbrig, siegeljb, annastef@umich.edu).*

Abstract: With the increased pervasiveness of Lithium-ion batteries, there is growing concern for the amount of retired batteries that will be entering the waste or recycling stream before they are fully utilized. Although aged batteries no longer meet the demands of their first application, many still have a significant portion of their initial capacity remaining for use in secondary applications, but evaluating this capacity is difficult and time intensive. In this paper, we investigate the use of cell (or parallel sets of cells) internal resistance as a surrogate of the capacity of parallel cells. We also highlight the challenges of testing batteries as a full pack despite the cell-to-cell variability from lack of balancing and differences in resistance and capacity. First, we verify that the charge-interrupt resistance from parallel cell pairs from twelve retired battery packs can eliminate the need for the hybrid pulse power characterization (HPPC) test as long as the charge-interrupt tests were not applied at low cell pair terminal voltages. Then, the relation between cell internal resistance and capacity across the various packs is investigated. Initial experimental results from this study show a correlation between internal resistance and remaining capacity which can be approximated with a linear fit, suggesting internal resistance measurements taken above a threshold cell pair terminal voltage may be a suitable initial screening metric for aged batteries.

Keywords: Diagnostics, Batteries, State of Health, Fault diagnosis, Monitoring

1. INTRODUCTION

The current exponential increase in the production of lithium-ion batteries for clean energy and electric vehicle applications will inevitably result in the presence of a large volume of "retired" batteries soon. Estimates from IEA (2020) suggest 100-120 GWh of EV batteries will be retired by 2030. Batteries are retired when they are unable to meet the original application's performance requirements. A battery pack for an electric vehicle, for instance, is warrantied to maintain 80% of its original capacity (Groenewald et al. (2017), Cusenza et al. (2019)) within ten years or 100,000 miles travelled. Retired batteries, while no longer able to meet performance standards of the the original application, still retain much of their performance capabilities in most cases and are sufficient to be applied in less-demanding applications (Zhu et al. (2021)). As such, to maximize the environmental and economic benefits of lithium-ion batteries, remanufacturing and repurposing is a key step in a battery's life-cycle (Hua et al. (2020)).

However, the cost of testing and refurbishing batteries is high and may prevent applications of retired batteries for second life from being economically viable (Rallo et al. (2020), Martinez-Laserna et al. (2018)). Neubauer et al. (2015) indicates the greatest portion of the testing and refurbishing cost is in labor costs, much of which is due to the time spent disassembling and testing a battery. A significant contributor to long test times is the assessment of a battery's state-of-health (SOH), which is a measure of a battery's current performance conditions compared to its original state. Changes in SOH is typically indicated by capacity loss, resistance increase, and occasionally involves changes in the open circuit voltage (OCV) with respect to state of charge (SOC) (Roscher et al. (2011)). However, obtaining the metrics of SOH involves slow charge and discharge testing on special equipment, which can take upwards of 20 hours to complete. Further, direct testing and repurposing batteries at the pack level typically requires active balancing and more time intensive measures of evaluating individual cells is required. As noted by Zhou et al. (2017), variations in individual cells making up a battery pack increase with aging of the pack and a few individual cells can reduce the performance of the entire pack. Thus, to develop a strategy that reduces testing time while providing an acceptable estimate of a cell's capacity, a metric for non-uniformities and the the worst cell SOH, typically determined by resistance and capacity, needs to be established. Significant reduction in the cost of testing batteries can make repurposing of retired batteries more economically feasible.

In Zhou et al. (2020), the current methods for evaluating retired or aged battery packs are segregated into two methodologies. The first focuses on the effectiveness and consistency of the evaluation process while neglecting time and effort considerations. An example of this is presented by Chung (2021) in which the standard method of evaluating the safety and performance of a retired battery is

conducted. The test procedure is defined by as outlined by the Underwriters Laboratories (UL) 1974 Standard. The second methodology, which is where this study aims to contribute, focuses on a surrogate for OCV that can be acquired faster than the current state of the art, 20+ hours, while still maintaining an acceptable level of consistency. Weng et al. (2013) propose a battery capacity estimation scheme that only needs charging data from 60%–85% SOC to estimate the battery capacity and avoids the need for a time-consuming full charge and discharge. Recent work by Mohtat et al. (2022) showed that this range of SOC provides critical information that correlates well with a cell's SOH, yet a full charge for one cell is typically required to reset SOC evaluation when the initial SOC is unknown. Zhou et al. (2020) used incremental capacity curves obtained with high charging current rates which are then used to extract approximations of capacity and internal resistance of cells. However, a full charge of the cells is still required despite occurring at a faster rate. Parametric studies from Barzacchi et al. (2022) further suggest an increase in internal resistance indicates degradation of the intercalation kinetics in a battery cell. While internal resistance is one of many parameters to influence the performance of a battery (Zhou et al. (2017)), it may be a rapid metric with which to initially screen retired batteries. Yet, even this simple metric can prove difficult to obtain in a fast and accurate manner when considering retired or discarded battery packs with no knowledge of the usage history. For instance, imbalance of cell voltages within a pack leads to sampling of cell resistance at different voltage, and therefore SOC, levels. Additionally, external contact and bus bar resistances from cell or pack construction can be difficult to isolate from internal cell resistance.

The following study investigates relation between an estimated internal resistance parameter, R_s and the measured capacity of retired batteries while also highlighting the challenges of evaluating these metrics experimentally in a fast and accurate manner. In the following sections, the testing procedures used to find the cell capacity as well as to rapidly estimate internal resistance through charge interrupt procedures are provided. Additionally, a hybrid pulse power characterization (HPPC) test is conducted as a baseline to compare the internal resistance estimates. Then, these tests were performed on discarded DeWALT lithium-ion power tool battery packs and a discussion of the R_s characteristics is provided. From these results, a clear correlation between cell capacity and resistance is observed. Further, these results hold across mid to high range terminal voltage values. This evaluation technique can then be used once surpassing a threshold cell terminal voltage without any knowledge of SOC, providing a fast initial screening test for aged Lithium-ion batteries.

2. CASE STUDY

The battery packs used in this study were DeWalt 20 V, 5 A-h model DCB205 lithium ion power tool battery packs, with a total of thirteen battery packs analyzed. An image of the pack as well as a schematic of the 2P5S cell arrangement within the pack is provided in Fig. 1. Each cell is an 18650 cylindrical cell with a capacity of 2.5Ah. It should be noted here that throughout the rest of the

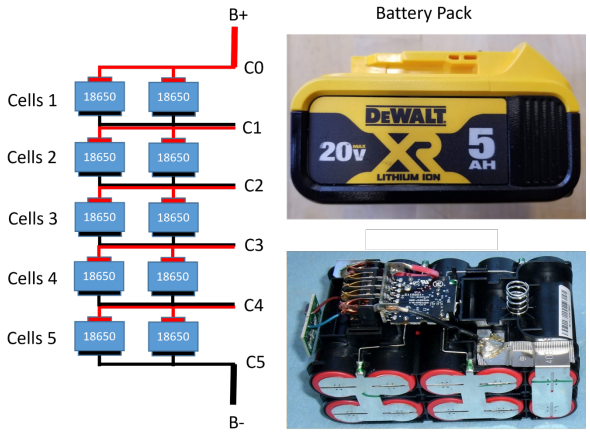

Fig. 1. Schematic of the 2P5S test setup along with an image of the battery pack and cell orientation within the pack.

paper, evaluation will be made of cell pairs 1-5 as shown in Fig. 1 rather than single cells. The decision to evaluate the parallel pairs was made because of the access to voltage measurements across the cell pairs. This was possible due to the pack hardware and greatly simplified deconstruction of the packs for testing and reduced testing time.

Twelve of the packs are considered aged and were acquired from a recycling center after consumers discarded them, presumably when deemed past their usable lifespan. The use and cycling history of these batteries are unknown. A fresh pack was purchased to act as a control test. The aged packs were grouped according to the two primary ID codes found, being N330105, which was determined to contain Samsung INR18650-25R cells with an NCA chemistry, and N437615 which contained LG LGABHE21865 cells with an NMC chemistry. Additionally, the new pack had an ID code of N522573 which also contains cells manufactured by LG with an NMC chemistry. In the following discussions, letters are used to denote the various packs. Pack A denotes the fresh pack while all other letters are the retired packs.

3. EXPERIMENTAL SETUP

The tests sequences and data acquisition were completed with an A&D iTest Test Cell System. The iTest System has an analog input module used for acquisition of the individual cell pair data voltage. A Bitrode FTV-1 Power Module controlled by the iTest system was the source of the voltage and current profiles.

The following sections outline the main testing procedures for the battery packs followed by an additional HPPC sequence. The estimated resistance parameters from the discharge interrupt, charge interrupt, and HPPC are compared to demonstrate the validity of the more rapid diagnostic procedure of interrupting a charge or discharge without providing that battery an extended rest period. The parameter of interest here is the ohmic resistance, R_s, which is responsible for the instantaneous voltage change when the cell pair is under load.

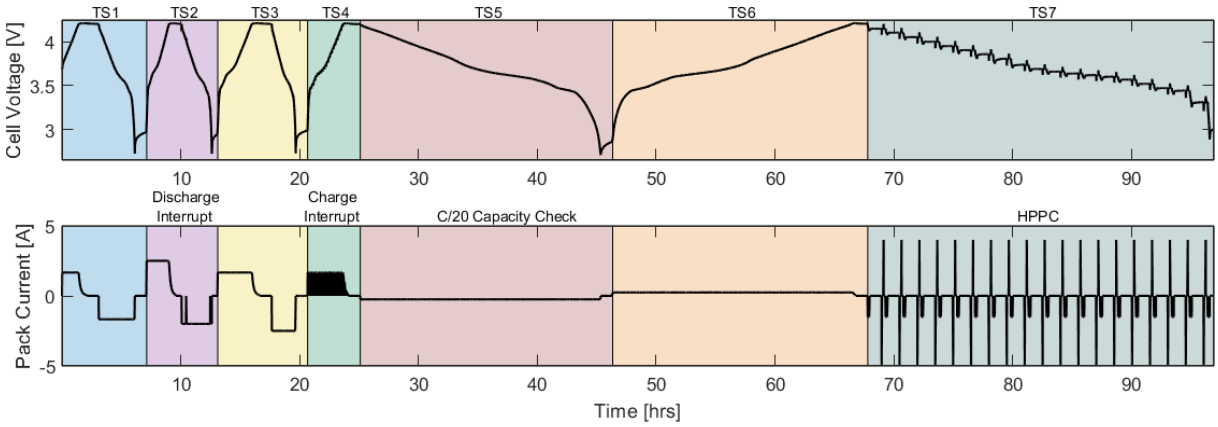

Fig. 2. cell pair Voltage and pack current profiles used for full characterization of each battery pack. Test sequences (TS) 1-6 are described in Tab. 1 and the discharge interrupt of TS2, charge interrupt of TS4, and HPPC of TS7 are detailed in section 3.1.

Table 1. Key details for each test sequence.

	Charge Rate	Discharge Rate
TS1	C/3	C/3
TS2	C/2	C/2.5
TS3	C/3	C/2
TS4	C/3 w/ interrupt	N.A.
TS5	N.A	C/20
TS6	C/20	N.A.
TS7	N.A.	C/3.33 w/ interrupt

3.1 Testing Procedure

The cell pair voltage and pack current profile initially used for evaluation of each battery pack is shown in Fig. 2. The profile can be separated into seven distinct test sequences (TS), labeled above the figure, with a 30 minute rest period between each individual test. The parameters for each sequence are listed in Tab. 1. The charge and discharge rate for each sequence are listed as C-rates, with the units of h^{-1} and defined as $C \equiv \frac{I}{Q_p}$ where I is the current required to charge or discharge the pack ampere hour capacity Q_p in the specified time. In TS1, an initial charge and discharge is completed for initial cycling of the pack as the initial state of charge (SOC) is unknown. The TS2 contains two current interrupts, which will be reffered to as discharge interrupts, occuring at 4V and 3.2V, to provide a means of calculating $R_{s,DI}$ from the instantaneous voltage change as

$$R_s = \frac{\Delta V_s}{\Delta I} \tag{1}$$

where V_s is considered to be the instantaneous voltage change when current is interrupted. During these discharge interrupts, the sampling rate is 1 Hz. The following TS3 simply provides an additional charge and discharge to isolate TS2 from TS4. In TS4, a charge interrupt procedure is completed across a range of voltages with a sampling rate of 10 Hz. A charging rate of $C/3$ is interrupted at 560 second intervals during which the current is set to 0 for 20 seconds. This allows $R_{s,CI}$ to be calculated over a range of cell pair voltages again using (1).

The purpose of TS5 is to find the capacity of each cell pair. Ideally, each charging profile is meant to follow a constant current, constant voltage (CCCV) charging strategy. From this fully charged initialization point in TS5, coulomb

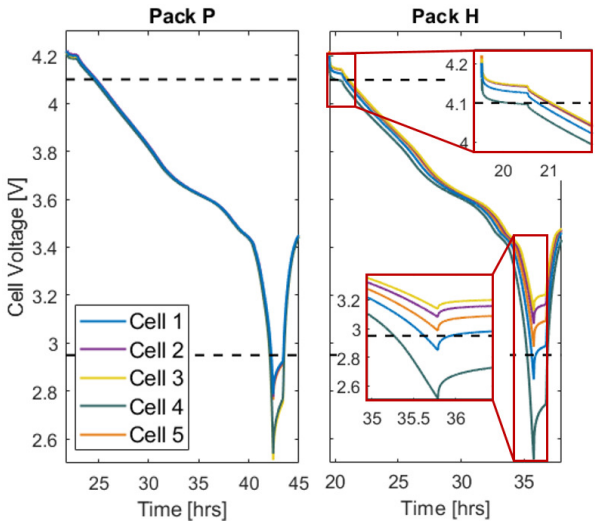

Fig. 3. Comparison of cell pair voltages within a single pack for packs P and H during TS5. Significant imbalance in the cell pair voltage requires the capacity to be evaluated between voltage points of 4.1V and 2.95V rather than the maximum and minimum voltage range of the cell pairs.

counting could be utilized to find cell pair capacity during the slow discharge of TS5. This slow discharge reduces the impact of internal resistance and concentration gradients on the measured terminal voltage, allowing for an accurate estimate of capacity by assuming the measured terminal voltage approximates the open circuit voltage (OCV) of the battery. However, due to imbalances in the individual cell pair voltages as the battery pack relies on an external balancing circuit, constant voltage charging could not always be achieved. This then changed the minimum voltage each cell pair reached during the discharge as shown in Fig. 3 where the discharge is stopped as soon as a single cell pair reaches the set minimum voltage. Figure 3 compares the cell pair voltage profiles for pack P as well as pack H. Due to the rapid change in cell pair voltage at low SOC, even small imbalances in the cell pairs results in a large difference in the capacity calculation when using the minimum and maximum terminal voltage. Therefore, capacity is still measured using coulomb counting, but only

between voltage set points of 4.1V and 2.95V. It should be noted that pack H is so imbalanced that only the capacity of cell pair 4 could be evaluated even using this modified method.

All packs also underwent an HPPC testing sequence, TS7, where each cell pair was subjected to a series of 10-minute C/3.33 constant-current discharge pulses, followed by a 60-minute rest period. This test was chosen as it provides a benchmark industry standard test procedure for characterizing the batteries internal resistance parameters (Zhang et al. (2011)). Figure 4 provides cell pair 2's voltage response from pack M to the current pulses of the HPPC testing sequence which was recorded at a rate of 10 Hz. At every discharge pulse, $R_{s,HPPC}$ was calculated using (1). The response of the voltage to a step change in current during the HPPC test is shown in Fig. 4, with the change in voltage due to the ohmic resistance denoted as ΔV_s.

The methods utilized to calculate $R_{s,DI}$, $R_{s,CI}$, and $R_{s,HPPC}$ from a step change in current are identical. Yet, should be noted that while these methods attempt to capture the instantaneous voltage change, it is unavoidable that time will elapse between the discrete sampling points, therefore capturing some of the more rapid diffusion dynamics in the R_s value. As the sampling times when finding $R_{s,CI}$ and $R_{s,HPPC}$ are identical, a direct comparison of these results is valid. However, the larger sample time used when calculating $R_{s,DI}$ increases the resistance value.

4. RESULTS AND DISCUSSION

The following sections present the R_s parameters calculated from the introduced test sequences and outline the possible efficacy of the R_s parameter in the estimation of the remaining capacity of a lithium-ion battery. The characteristics of R_s over a range of terminal voltages is discussed along with a comparison of the R_s parameters calculated by the charge interrupt and HPPC test sequences as well as a brief discussion of the discharge interrupt results to convey the importance of a standardized sampling time when implementing this method. Additionally, the apparent linear relation between R_s and battery capacity, a key factor of the SOH the battery, is introduced despite the relatively small sample set of aged batteries in this study.

4.1 Series Resistance Parameters

As the HPPC test sequence provides a benchmark to the industry standard practice for parameterizing internal resistance in batteries, a comparison between the $R_{s,HPPC}$ calculated from the HPPC test and the $R_{s,CI}$ calculated from the charge interrupt is provided in Fig. 5 for cell pair 4 in three different aged battery packs. As noted previously, only the capacity in cell pair 4 could be measured due to large cell pair imbalance. Therefore, cell pair 4 is mainly used for comparison in the following discussion. The packs C and J were chosen as pack C contains cells manufactured by LG, while pack J contains cells manufactured by Samsung. In addition, pack H was included as this pack showed much more significant signs of aging as compared to the rest of the packs studies, as will be discussed later.

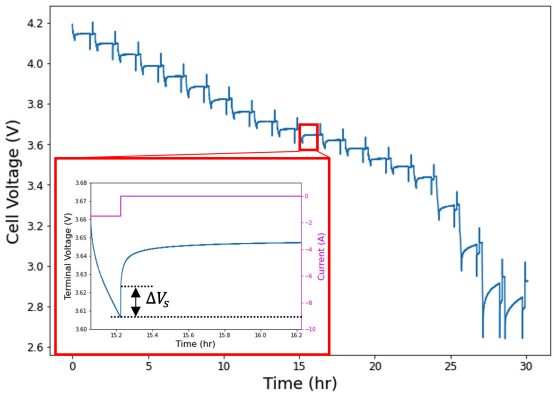

Fig. 4. Profile of cell pair 2's voltage in pack M during the HPPC test sequence. During each interrupt of the discharge current, the instantaneous as well as total voltage change of the cell pair is recorded to calculate the internal resistance parameters.

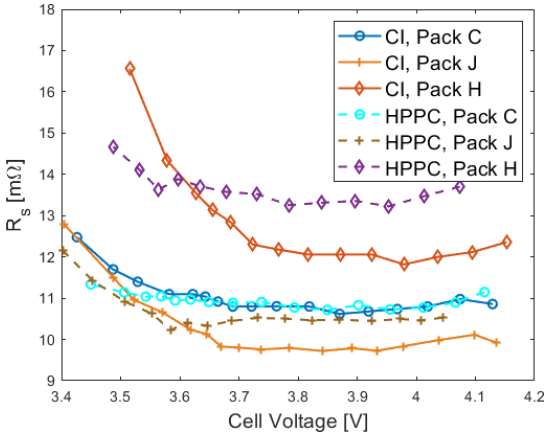

Fig. 5. Results of the R_s calculations for the charge interrupt (CI) and HPPC test sequences for cell pair 4 in battery packs C, J, and H. Both tests can easily identify pack H as having significantly higher resistance compared to packs C and J.

From Fig. 5 it is apparent that while there is not perfect alignment of the results from the charge interrupt and HPPC tests, the trend in R_s between the different packs is maintained. The resistance calculated in the cell pair from pack H is considerably larger than that of packs C and J. It should also be noted that while each testing sequence calculates R_s in a similar manner, the charge interrupt was completed during charging of the battery while the HPPC test was completed during a discharge, which may account for some of the difference in R_s values. Furthermore, as the HPPC test attempts to characterize not only the ohmic resistance R_s but also the dynamic resistance, an extended rest period is required, resulting in a test lasting approximately 30 hours in this case. The charge interrupt test lasted only 3 hours, an order of magnitude reduction in time required to complete the test. Furthermore, the R_s values are relatively constant at mid and high values of the cell pair terminal voltage. While there is a gradual increase at low voltages, typically around 3.6V or lower, this lower voltage range makes up a significantly smaller portion of the operating range due to the rapid voltage drop near low SOC. As such, single charge interrupts after

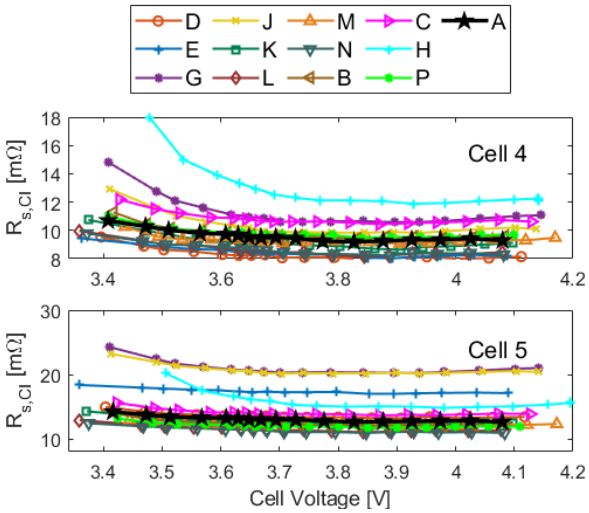

Fig. 6. Values of R_s for cell pairs 4 and 5 in a battery pack. Values are taken from charge interrupt test for all thirteen pack analyzed with the fresh pack denoted by A. cell pair 5 is on the exterior of the pack while cell pair 4 is on the interior.

charging to a voltage threshold of approximately 3.6V can provide a rapid approximation for the R_s parameter of a cell pair.

In Fig. 6, the $R_{s,CI}$ values from the charge interrupt tests are provided for cell pairs 4 and 5 from all the packs analyzed. These cell pairs were selected for this figure as cell pair 5 is a pair on the exterior of the pack and connected to the pack tabs, while 4 is in the interior of the pack, as shown in the pack schematic in Fig. 1. The trend of increases $R_{s,CI}$ at lower SOC is observed for all packs, including the fresh pack denoted as A. However, the increase of $R_{s,CI}$ in cell pair 5 shows a significant departure from the resistance values measured in pair 4. Referring back to the pack schematic provided in Fig. 1, it is assumed that the increase in resistance is not entirely due to internal resistance of cell pair 5. Rather, the external resistance of the tabs denoted by $B+$ and $B-$ in Fig. 1 may be responsible for a significant portion of the resistance increase. The interior cell pairs 2, 3, and 4 are isolated from this issue as the tabs used to measure the terminal voltage are not current carrying. Further experiments are required to isolate the true internal resistance of pairs 1 and 5 from the external tab resistance. All of the following discussion will focus on the results from cell pairs 2, 3, and 4.

From Fig. 5 and 6, pack H has a noticeably higher resistance than most packs in cell pair 4, followed by packs C and G. The other aged packs are more densely populated around the fresh pack A. As the objective of this study is to analyze the ability of R_s to provide an indication of the capacity, a defining metric of SOH, these differences in R_s are next presented with respect to the measured capacity of each pack.

4.2 Capacity and Series Resistance

As outlined in section 3.1, the capacity of the battery packs are calculated between the voltage limits of 2.95V and

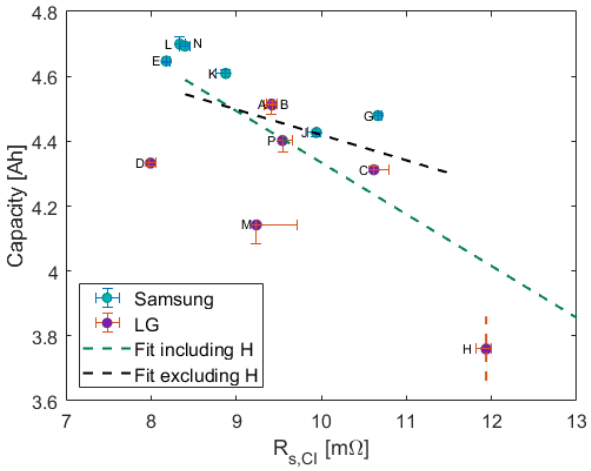

Fig. 7. Capacity and resistance for each pack for cell pair 4. The bars associated with each point denote the range of resistance and capacity associated with pairs 2-4 in each pack. The uncertainty in the range of capacity in pack H due to cell pair imbalance is highlighted by a dashed red bar.

4.1V during the the C/20 discharge in TS5, which takes upwards of 20 hours for each pack. In Fig. 7, the capacity of cell pair 4 is shown with respect to the corresponding ohmic resistance $R_{s,CI}$. The $R_{s,CI}$ value used from each pack was the sample point closest to a terminal voltage of 4V. The bars associated with each point denote the range of resistance and capacity associated with cell pairs 2-4 in each pack. However, due to the large cell pair imbalance in pack H shown in Fig. 3, the capacity between voltage limits of 2.95V and 4.1V was not able to be calculated for cell pairs 2 and 3. This lack of range quantification is denoted by the dashed bar in Fig. 7. While there is a limited sample size provided for this comparison, the overall relation between capacity and $R_{s,CI}$ can initially be approximated by a linear fit. As mentioned previously, pack H has the highest measured resistance, and this corresponds to the lowest measured capacity for all of the cell pairs. Similarly, pack E, L and N have some of the lowest resistances and highest measured capacities, even higher than that of the fresh pack. However, pack M displays the second lowest capacity while having a resistance almost identical to that of fresh pack A, limiting somewhat the linear relationship between capacity and resistance, along with pack D.

The proposed linear relationship between R_s and capacity can potentially be explained from a lithium inventory loss perspective as detailed by Prasad and Rahn (2013). The solid electrolyte interphase (SEI) layer is an electrically insulating film on the negative graphite electrode in a lithium-ion cell, protecting the electrode from the solvents in the electrolyte. While this layer is largely permeable to lithium ions, the SEI layer will slowly consume lithium as the cell cycles and is considered a major factor in capacity loss for lithium ion batteries. As the SEI layer grows and consumes more lithium, the SEI thickness increases, increasing the internal resistance of the cell and causing more power to be lost (Plett (2015)).

A linear fit including all of the packs obtains an R^2 value of 0.50, which means 50% of the variance in the data can

be explained by the linear fit. While this is a relatively low metric for the goodness of fit, it should be noted that none of the aged pack meet the 80% capacity metric typically considered for classifying automotive battery packs as below the range of the warranty. Further, if we eliminate pack H from the fit, the general slope of the line is maintained, as shown in Fig. 7, but the R^2 value drops to 0.26 due to the limited range of pack capacity. This suggests further analysis with a wide range of aged cells are required to experimentally substantiate the capacity-resistance relationship.

5. CONCLUSIONS

This paper is motivated by the current practice of evaluating starting, lighting and ignition (SLI) lead-acid batteries that use resistance as a metric of battery SOH to explore a similar correlation in lion-batteries that are used in power applications. To this end, we investigated the correlation of of ohmic resistance, R_s, to the remaining capacity in a lithium-ion cell pair. From the thirteen battery packs analysed, $R_{s,CI}$ provides an approximately linear indication of capacitance without the necessity of performing 20 hours-long discharge protocol that is currently used to evaluate the cell pair capacity. Further, $R_{s,CI}$ remained constant for mid to high range terminal voltage values, eliminating the need for an exact knowledge of SOC when utilizing $R_{s,CI}$ as a capacity metric.

Future work will expand and verify the finding to other packs in power tools, scooters, ebikes and aged packs from retired electric buses. We will also test the individual cells rather than cell pairs to quantify their variability in capacity and resistance to substantiate values we have found when testing under the limitations of cell pair testing.

ACKNOWLEDGEMENTS

The authors would like to acknowledge the support of Paul Hernley from Battery Solutions, LLC who provided the used battery packs from their recycling facility.

REFERENCES

Barzacchi, L., Lagnoni, M., Rienzo, R.D., Bertei, A., and Baronti, F. (2022). Enabling early detection of lithium-ion battery degradation by linking electrochemical properties to equivalent circuit model parameters. *Journal of Energy Storage*, 50, 104213. doi: 10.1016/j.est.2022.104213.

Chung, H.C. (2021). Charge and discharge profiles of repurposed LiFePO4 batteries based on the UL 1974 standard. *Sci. Data*, 8(1). doi:10.1038/s41597-021-00954-3.

Cusenza, M.A., Guarino, F., Longo, S., Mistretta, M., and Cellura, M. (2019). Reuse of electric vehicle batteries in buildings: An integrated load match analysis and life cycle assessment approach. *Energ Buildings*, 186, 339–354. doi:10.1016/j.enbuild.2019.01.032.

Groenewald, J., Grandjean, T., and Marco, J. (2017). Accelerated energy capacity measurement of lithium-ion cells to support future circular economy strategies for electric vehicles. *Renewable Sustainable Energy Rev.*, 69, 98–111. doi:10.1016/j.rser.2016.11.017.

Hua, Y., Zhou, S., Huang, Y., Liu, X., Ling, H., Zhou, X., Zhang, C., and Yang, S. (2020). Sustainable value chain of retired lithium-ion batteries for electric vehicles. *J Power Sources*, 478, 228753. doi: 10.1016/j.jpowsour.2020.228753.

IEA (2020). *Global EV Outlook 2020: entering the decade of electric drive?* IEA Publications. doi: 10.1787/d394399e-en.

Martinez-Laserna, E., Gandiaga, I., Sarasketa-Zabala, E., Badeda, J., Stroe, D.I., Swierczynski, M., and Goikoetxea, A. (2018). Battery second life: Hype, hope or reality? a critical review of the state of the art. *Renewable Sustainable Energy Rev.*, 93, 701–718. doi: 10.1016/j.rser.2018.04.035.

Mohtat, P., Lee, S., Siegel, J.B., and Stefanopoulou, A.G. (2022). Comparison of expansion and voltage differential indicators for battery capacity fade. *J Power Sources*, 518, 230714. doi:10.1016/j.jpowsour.2021.230714.

Neubauer, J., Smith, K., Wood, E., and Pesaran, A. (2015). Identifying and overcoming critical barriers to widespread second use of PEV batteries. Technical report. doi:10.2172/1171780.

Plett, G. (2015). *Battery management systems, Volume 1: Battery Modeling*, volume 1. Artech House, Norwood.

Prasad, G.K. and Rahn, C.D. (2013). Model based identification of aging parameters in lithium ion batteries. *J Power Sources*, 232, 79–85. doi: 10.1016/j.jpowsour.2013.01.041.

Rallo, H., Benveniste, G., Gestoso, I., and Amante, B. (2020). Economic analysis of the disassembling activities to the reuse of electric vehicles li-ion batteries. *Resources, Conservation and Recycling*, 159, 104785. doi: 10.1016/j.resconrec.2020.104785.

Roscher, M.A., Assfalg, J., and Bohlen, O.S. (2011). Detection of utilizable capacity deterioration in battery systems. *IEEE Trans. Veh. Technol.*, 60(1), 98–103. doi: 10.1109/tvt.2010.2090370.

Weng, C., Cui, Y., Sun, J., and Peng, H. (2013). On-board state of health monitoring of lithium-ion batteries using incremental capacity analysis with support vector regression. *J Power Sources*, 235, 36–44. doi: 10.1016/j.jpowsour.2013.02.012.

Zhang, Y., Wang, C.Y., and Tang, X. (2011). Cycling degradation of an automotive LiFePO4 lithium-ion battery. *J Power Sources*, 196(3), 1513–1520. doi: 10.1016/j.jpowsour.2010.08.070.

Zhou, L., Zheng, Y., Ouyang, M., and Lu, L. (2017). A study on parameter variation effects on battery packs for electric vehicles. *J Power Sources*, 364, 242–252. doi:10.1016/j.jpowsour.2017.08.033.

Zhou, Z., Duan, B., Kang, Y., Shang, Y., Cui, N., Chang, L., and Zhang, C. (2020). An efficient screening method for retired lithium-ion batteries based on support vector machine. *J Clean Prod*, 267, 121882. doi: 10.1016/j.jclepro.2020.121882.

Zhu, J., Mathews, I., Ren, D., Li, W., Cogswell, D., Xing, B., Sedlatschek, T., Kantareddy, S.N.R., Yi, M., Gao, T., Xia, Y., Zhou, Q., Wierzbicki, T., and Bazant, M.Z. (2021). End-of-life or second-life options for retired electric vehicle batteries. *Cell Reports Physical Science*, 2(8), 100537. doi:10.1016/j.xcrp.2021.100537.